TITLE: Proximal ganglionic intestine in Hirschsprung Disease is fibrotic and stiff

AUTHORS: Prisca C. Obidike[1,*]; Britney A. Hsu[2,3,*]; Chioma Moneme[1]; Oluyinka O. Olutoye II[2]; Walker D. Short[2]; Hui Li[2,3]; Swathi Balaji[2,3]; Yuwen Zhang[1]; Sundeep G. Keswani[2,3]; Lily S. Cheng[1,2,3]

[1] Division of Pediatric Surgery, Department of Surgery, University of Virginia, Charlottesville, VA, USA
[2]Department of Surgery, Baylor College of Medicine, Houston, TX, USA
[3]Division of Pediatric Surgery, Department of Surgery, Texas Children's Hospital, Houston, TX, USA
[*]These authors contributed equally

Correspondence: Lily S. Cheng

Email address: lilycheng@virginia.edu

Address: 409 Lane Rd, Charlottesville, VA 22903

Tel: 408-318-0900

Conflict of Interest statement:

The authors have declared that no conflict of interest exists.

ABSTRACT

Hirschsprung disease (HSCR) is a congenital intestinal disorder characterized by the absence of ganglia in the distal intestine. Despite surgical resection of the aganglionic intestine and pull-through surgery, HSCR patients still experience bowel dysfunction, indicating that latent abnormalities may also exist in the proximal ganglionic intestine. To elucidate possible causes of postoperative bowel dysfunction in HSCR, we investigated differences in the proximal ganglionic intestine using an animal model of HSCR (*Ednrb*-null mice) and validated our findings in tissue from human HSCR patients. We found that the proximal ganglionic colon of HSCR mice exhibited greater stiffness and fibrosis than their wild-type littermates. Similarly, submucosal fibrosis was significantly greater in the proximal ganglionic intestine of HSCR patients than in intestinal tissue from age and site-matched controls. Furthermore, we observed dysregulated expression of extracellular matrix (ECM)-related genes in the proximal ganglionic intestine of HSCR mice compared to controls. We conclude that increased fibrosis, stiffness, and alterations in ECM composition may contribute to persistent dysfunction of the ganglionic intestine in HSCR. These findings add to the growing body of literature that describe abnormalities in the proximal ganglionic intestine of HSCR and suggest that HSCR is not limited to the aganglionic intestine alone.

INTRODUCTION

The enteric nervous system (ENS) is a complex network of neurons and glia within the gastrointestinal (GI) tract that regulates gut motility and homeostasis independently of the central nervous system (1–4). The ENS is derived from enteric neural crest cells (eNCC), which migrate caudally from the vagal neural tube to colonize the developing gut (5,6). Disruption of eNCC migration can lead to disorders such as Hirschsprung disease (HSCR) (7,8). HSCR, a congenital GI disease that affects 1 in 5,000 live births, is characterized by a complete absence of ganglia in the distal intestine (2,9). The current standard of care is surgical resection of the aganglionic intestine and pull-through of the ganglionic intestine (10,11). However, even after successful surgery, more than half of patients experience persistent bowel dysfunction, including chronic constipation, fecal incontinence, and Hirschsprung-associated enterocolitis (HAEC), a leading cause of morbidity and mortality in this population (7,11,12). The persistence of bowel dysfunction despite surgical resection of the aganglionic intestine suggests that latent abnormalities may also be present in the proximal ganglionic intestine.

The GI microenvironment, particularly the extracellular matrix (ECM), plays a critical role in ENS development by guiding eNCC migration, proliferation, and differentiation along the GI tract (8,13–15). The ECM, a three-dimensional acellular structure composed of collagens, glycoproteins, and proteoglycans, provides structural support and biochemical cues essential for coordinated ENS development (8,13). Alterations in ECM components such as laminin and collagen have been observed in ganglionic segments of HSCR intestine and may contribute to its pathogenesis (16,17). Importantly, ECM composition also governs tissue mechanical properties, such as stiffness, which also influence eNCC behavior during development (18). Although ECM remodeling continues after birth (13), the ECM composition and biomechanical properties of postnatal HSCR intestine remain poorly characterized. To identify potential contributors to HSCR-related bowel dysfunction, we investigated ECM composition and mechanical properties in the proximal ganglionic intestine of HSCR. We hypothesized that both are altered in HSCR compared to normal intestine.

To test this, we used *Ednrb*$^{-/-}$ mice, a widely accepted animal model of HSCR that exhibits distal aganglionosis of the colon similar to the most common phenotype of human HSCR (19–21). We assessed the mechanical properties and ECM composition of the proximal ganglionic intestine in these mice and validated these findings using resected bowel from HSCR patients. To determine whether observed differences were due to disease-specific pathology or a consequence of bowel distention, we also analyzed distended intestinal tissue patients with intestinal atresia. Our findings contribute to the growing body of evidence suggesting that the proximal ganglionic intestine in HSCR is not entirely normal and may play a role in postoperative bowel dysfunction.

RESULTS

The Proximal Ganglionic Colon in HSCR Mice is Stiff and Fibrotic

Masson's trichrome staining was performed on proximal ganglionic mouse colon to examine collagen content in the muscularis propria layer. Normoganglionosis was confirmed by IHC for the pan-neuronal marker, Tuj1 (Figure 1 A-F). Histological analysis of representative images showed greater collagen deposition, represented in blue by Masson's trichrome staining, in the proximal ganglionic colon of HSCR mice (n = 12) compared to equivalent proximal colon segments of their WT littermates (n = 12) (Fig. 2A-B). Quantification of collagen deposition in both groups showed that HSCR mice had greater collagen content in the proximal colon than their WT littermates (116.92 ± 13.76 vs. 108.04 ± 13.65, p = 0.006, Fig. 2C). Similarly, the collagen content in the distal colon of the WT mice was significantly greater than the distal colon of HSCR mice (111.90±10.83 vs. 86.156 ± 11.32, p = 0.025).

Atomic force microscopy (AFM) was used to examine the stiffness of the colonic tissue from HSCR and their WT littermates. The elastic modulus, which represents the stiffness, is the force required to deform these tissues. The AFM cantilever probe was brought in contact with the muscularis propria layer as identified by microscopy, and the elastic modulus was obtained. We observed that the proximal colon of HSCR was significantly stiffer than that of WT mice (25.29 ± 11.96 vs. 18.17 ± 9.31 kPa, p = 0.015, Fig. 2D).

Dysregulation of Extracellular Matrix-Related Genes in HSCR Proximal Ganglionic Colon

Bulk RNA sequencing was performed to examine the relative expression of ECM-related genes in the proximal colon of HSCR compared to WT mice (Figure 3A). RNA was extracted from homogenized LMMP samples obtained from the freshly dissected proximal colon and sequenced to construct a polyA enrichment library. Differential expression analysis demonstrated 1,012 genes uniquely dysregulated in the proximal colon of HSCR mice, 908 unique to WT littermates, and 11,846 genes shared between both groups (Figure 3B). A volcano plot comparing gene expression between HSCR and WT proximal colon identified 1,009 genes were upregulated and 1,099 genes were downregulated (log2FC > ± 1, padj < 0.05) (Figure 3C). Kyoto Encyclopedia of Genes and Genomes (KEGG) enrichment analysis revealed statistically significant differences in pathways related to neuroactive ligand-receptor interaction and cell adhesion molecules between HSCR and WT mice (Figure 3D).

We also queried differentially expressed genes specifically for genes involved in focal adhesion (mmu04510) (22), ECM-receptor interaction (mmu04512) (23), neuroactive ligand-receptor interactions (mmu04080) (24), ECM (25), and fibrosis (26) (Supplemental Table 1).Of the 62 individual genes in these pathways, 10 were significantly up- or down-regulated (padj < 0.05) (Figure 4A-B). Specifically, the proximal ganglionated colon of HSCR mice demonstrated increased expression of genes encoding Thrombospondin 4 (*Thbs4*), matrix metallopeptidase 7 (*Mmp7*), and Syndecan-1 (*Sdc1*). Downregulated genes included Vascular cell adhesion molecule 1 (*Vcam1*), Collagen type IX, alpha 2 subunit (*Col9a2*), Opioid receptor kappa 1 (*Oprk1*), Solute carrier family (sodium-dependent inorganic phosphate cotransporter) member 6 (*Slc17a6*), Tachykinin 1 (*Tac1*), Preproenkephalin (*Penk*), and Solute carrier family 5 (choline transporter) member 7 (*Slc5a*) (Figure 4B).

Ganglionic Intestinal Tissue of HSCR Patients is Fibrotic

To validate our findings in humans, we obtained intestinal tissue specimens from patients with HSCR (n = 6) and age-matched controls (n = 3) with no history of congenital colorectal disease who underwent bowel resection, ostomy formation, or ostomy closure (Table 1). Intestinal tissues were examined with Masson's trichrome staining to quantify collagen content in the muscularis propria and the submucosa (Figure 5A-D). Notably, the collagen content in the submucosa was significantly greater in the ganglionic intestinal

tissue of HSCR patients compared to equivalent segments from control patients (184.91 ± 34.30 vs. 133 ± 27.02, p = 0.001; Figure 5E- F). In contrast, there was no significant difference in the collagen content of the muscularis propria between HSCR and control patients (186.40 ± 37.92 vs. 148.45 ± 53.14, p = 0.082).

Comparison of Fibrosis in HSCR, Intestinal Atresia and ARM

To determine whether fibrosis in the proximal ganglionic colon in HSCR is due to disease-related pathology or secondary to chronic intestinal distention, we compared collagen content between distended proximal and non-distended distal intestine in patients with intestinal atresia (Table 1). There were no significant differences in the collagen content in either submucosa (168.42 ± 8.61 vs. 160.43 ± 5.35, p = 0.103) or muscularis propria (186.99 ± 10.21 vs. 194.43 ± 15.94, p = 0.154) of the distended and non-distended intestine in patients with intestinal atresia (Figure 6 E-F).

To further assess whether intestinal fibrosis was specific to HSCR, we quantified fibrosis in age- and site-matched tissues from patients with HSCR and ARM. Patients with ARM were chosen as they were the closest age and tissue match for younger HSCR patients. No significant differences in the collagen content in either the submucosa (80.42 ± 12.39 vs. 76.64 ± 6.82, p= 0.373) or the muscularis propria were observed (102.78 ± 9.08 vs. 105.11 ± 6.02, p=6286) in the HSCR compared to ARM tissues (Figure 6 A-D).

DISCUSSION

When Harald Hirschsprung first described Hirschsprung disease in 1886, he believed that dilation of the proximal colon was the main cause of disease (27). Only a decade later did Karl Tittel recognize that Hirschsprung disease was actually due to aganglionosis of the distal colon, leading to the surgical treatments that are the standard of care today (28). However, despite resection of the aganglionic intestine and pull-through of the ganglionated intestine, many HSCR patients continue to experience bowel dysfunction. The cause of this dysfunction is not fully known, but suggests--as Dr. Hirschsprung originally believed--that underlying abnormalities exist in the proximal ganglionated intestine. Our results show that the proximal ganglionated colon is stiff and fibrotic with dysregulated ECM composition.

Previous studies have identified abnormalities within the ganglionated intestine in HSCR. Specifically, altered neuronal density, neurotransmitter expression, and dysmotility have been noted in the ganglionic region of the *Ednrb*$^{-/-}$ mouse (1,20). Similar findings have been validated in human patients with HSCR and found to correlate with clinical outcomes (29,30). Abnormalities in the microenvironment of the ganglionated colon have also been described. Deviations in ECM composition of the gut during development are noted to contribute the pathogenesis of HSCR (8,31–33). Notably, increased expression of collagen VI has been found in the ganglionic colon of HSCR patients, especially HSCR patients with Down syndrome, and collagen VI is thought to interfere with normal eNCC migration to contribute to the pathogenesis of HSCR. An increased expression of collagen I and III and decreased expression of collagen IV in the proximal colon relative to the distal colon has also been described (14). In our study, we describe for the first time that overall collagen content, manifested as fibrosis, is significantly greater in ganglionated HSCR intestine compared to normal intestine. These findings add incremental knowledge to a growing body of evidence suggesting that the ganglionic HSCR intestine is not as normal as once believed.

The cause of fibrosis and ECM dysregulation in HSCR is not known, but we hypothesized that it may be secondary to chronic distention of the ganglionic region. Mechanical tension has been mechanistically linked to fibrosis in other organ systems (34–37). The ECM is considered a viscoelastic material that exhibits both viscous characteristics, evidenced by its ability to deform gradually without full recovery, and elastic properties, demonstrated by immediate deformation with the capability to return to its original shape when exposed to mechanical stress (36,38,39). Thus, the ECM surrounding intestinal cells remodels constantly to absorb the mechanical forces that occur during digestion and elimination. In the proximal ganglionated bowel, which is subject to significant distention in HSCR, the ECM may be altered to support tissues under greater mechanical stress. Interestingly, however, we noted no significant fibrosis in another model of intestinal distention, congenital intestinal atresia. This may be due to disease-specific differences in atresia compared to HSCR. In intestinal atresia, a vascular insult in utero disrupts intestinal continuity, leading to intestinal obstruction and proximal bowel distention, but ENS structure and function are normal (40). Altered wound healing and reduced fibrosis in the fetal environment in intestinal atresia may also contribute (41,42). The absence of increased fibrosis in the distended segment proximal to the atretic area may also reflect that surgical repair typically occurs shortly after birth, as seen in the younger age of our patient cohort. Consequently, the brief duration of obstruction may not allow sufficient time for chronic tissue remodeling to develop. Another contributing factor may be the limited sample size and use of small intestine rather than colonic tissue for analysis. Our lab is currently developing a postnatal model of chronic intestinal distention to better determine if fibrosis is secondary to distention or specific to HSCR. Alternatively, fibrosis in the ganglionic HSCR intestine may due to inflammation, such as HAEC (43), or prior surgery. While we did not explore the potential contribution of inflammation to intestinal fibrosis in this study, we note that no patients exhibited clinical signs of

HAEC at time of bowel resection and no tissue specimens were taken from a previous surgical site. Still, prior surgery and enterocolitis could influence tissue stiffness and fibrosis. To determine if HAEC is associated with fibrosis, future studies might examine fibrosis and ECM composition in patients with and without a history of HAEC.

Fibrosis is often associated with increased stiffness (44,45). Using atomic force microscopy (AFM), we measured that the stiffness of the proximal ganglionated colon of HSCR mice was approximately 1.4 times greater than equivalent intestinal segment from WT littermates. AFM is considered the gold standard for measuring mechanical properties of soft biological samples due to its ability to detect nanomechanical forces and precise spatial resolution without tissue deformation (46,47). Although there are numerous contributors to tissue stiffness, increased collagen content and collagen cross-linking are strongly associated with increased tissue stiffness (18,48,49). Our findings, and previous work by Chevalier et al (18), support the understanding that collagen, the most abundant ECM component, is a key contributor to tissue stiffness in the GI tract. Stiffness, as well as collagen content, plays a crucial role in eNCC migration during development (18). The effect of postnatal tissue stiffness and fibrosis on the ENS remains to be seen and is the subject of ongoing studies in our lab.

Limitations of this study include a small sample size of HSCR patients and controls. Thus, our study may be underpowered to detect a difference in fibrosis in the muscularis propria in human HSCR. Though each tissue specimen was matched for age and site, specimens encompassed a wide age range and varying intestinal locations. This was primarily due to the limited availability of appropriate controls. To eliminate potential confounding factors, we limited controls only to patients with no diagnosed GI or systemic disease, specifically, healthy patients who had intestinal resection for unexpected traumatic injuries. This resulted in an older cohort of HSCR patients in whom fibrosis may be more pronounced due to chronicity of symptoms. We separately compared a cohort of younger HSCR patients with age- and site-matched intestinal tissue from patients with ARM and found no difference in fibrosis; however, this may be due to confounding intestinal abnormalities in patients with ARM, who also experience chronic distention and dysfunction. Additionally, in younger patients (including patients with intestinal atresia), the absence of increased fibrosis in the distended segments may reflect an acute presentation with insufficient time for tissue remodeling to occur. Another important limitation is that nerve fiber hypertrophy, a key histological feature of aganglionosis, may vary with the extent of aganglionosis in both animal models and patients. This variation may potentially contribute to differences in tissue architecture. In our animal studies, the small number of significant ECM-related genes identified could also be due to sample size and within-sample heterogeneity. Additionally, we used trichrome staining, a widely accepted technique for quantifying collagen content in tissues, but we did not explore the differences in specific collagen types as has been done in previous studies. Lastly, though we did not measure stiffness of the ganglia directly, previous studies have found that the stiffness of the muscularis propria closely represents the stiffness of the ganglia (47).

In conclusion, our study demonstrates that the proximal ganglionated intestine in HSCR is stiff, fibrotic, and exhibits dysregulated expression of ECM-related genes. These abnormalities may contribute to the postoperative bowel dysfunction observed in HSCR patients.

MATERIALS AND METHODS

Sex as a Biological Variable

Our study included male and female animals and individuals. Similar findings are reported for both sexes.

Animal Subjects

Male and female heterozygous *Ednrb*^{tm1Ywa} mice on a hybrid C57BL6/J-129Sv background were purchased from the Jackson Laboratory (Bar Harbor, ME, USA) and bred to obtain homozygous (*Ednrb*$^{-/-}$) mice and wild-type (WT; *Ednrb*$^{+/+}$) mice. *Ednrb*$^{-/-}$ mice, commonly used as a model for human HSCR, have a disrupted endothelin-B-receptor gene that results in distal colonic aganglionosis and a pie-bald coat color, while their *Ednrb*$^{+/+}$ or $^{+/-}$ littermates appear phenotypically normal (21). Mice were genotyped by polymerase chain reaction to distinguish between *Ednrb*$^{+/+}$ or $^{+/-}$ mice. Two- to four-week-old mice were euthanized, and their entire colons were dissected and removed. The proximal ganglionic colon was delineated by gross colonic distention in *Ednrb*$^{-/-}$ mice and confirmed by immunohistochemistry for the pan-neuronal marker, Tuj1. Equivalent segments of proximal colon were collected from WT littermates.

Human Subjects

Ganglionic intestinal tissues were collected from two cohorts of patients with HSCR to enable age-matched comparisons. 1) Equivalent segments of intestinal tissue were collected from normal age-matched control patients with no prior history of systemic or intestinal disease who were undergoing stoma formation or closure after traumatic injuries (Control: n = 3; range 2 - 13 years vs. HSCR: n = 6; range 1 - 14 years old). 2) Additional samples were collected from patients with anorectal malformations (ARM: n=4, range 3 weeks - 10 months old vs. HSCR: n=5; range 9 days -2 years old).

Normoganglionosis was confirmed by histologic examination in all cohort tissues. Proximal and distal intestinal segments were also obtained from patients with intestinal atresia (n = 3; range 3 days to 2 months old) to compare fibrosis in distended and nondistended intestines without HSCR. The age and sex of all patients are listed in Table 1. This study was approved by the Baylor College of Medicine Institutional Review Board.

Histology and Immunohistochemistry

Colonic tissues from mice and human subjects were isolated and fixed in 10% formalin and embedded in paraffin in a standard histological fashion. Tissues in paraffin-embedded blocks were sectioned at a thickness of 5 µm using an RM 2235 Microtome (Leica Biosystems, Deer Park, IL, USA) and placed onto glass slides. Tissue sections were then de-paraffinized and rehydrated to PBS following standard protocol, and immunohistochemistry (IHC) staining was performed on a Dako Auto-stainer Link 38 (DakoLink version 4.1, edition 3.1.0.987; Agilent, Santa Clara, CA). Tissue sections were permeated with 1% BSA and 0.1% Triton X-100 in PBS for 1 hour, then incubated with the primary antibody, mouse anti-Tuj1 (1:500; GTX130245**,** GeneTex, Irvine, CA, USA) at 4°C for 24 to 48 hours. Then, tissues were washed in PBS and incubated with a secondary antibody, rabbit anti-mouse AlexaFluor 488 (1:1000; A27023, ThermoFisher, Waltham, MA, USA) at 4°C for 1 hour. Slides were mounted using a DAPI-containing mounting media (VectaShield Anti-fade mounting media; Vector Laboratories, Newark, CA, USA).

For hematoxylin and eosin (H&E) staining, tissue sections were stained using the SelecTech H&E system (Leica Biosystems) according to the manufacturer's instructions. For trichrome staining, tissue sections were stained using Masson’s trichrome special stain kit (Leica Biosystems) according to the manufacturer's instructions. Images were taken using a Leica DM500 or DMi8 microscope (Leica Biosystems).

Quantification of Collagen Content

Collagen content was quantified using trichrome-stained tissue sections. Collagen content was calculated using the color threshold tool in ImageJ (National Institutes of Health, Bethesda, MD, USA) according to previously published methods (11). For animal studies, the average collagen content was calculated from representative images of the colonic muscularis propria in the proximal and distal colon for *Ednrb*$^{-/-}$ mice and wild-type littermates (n = 12 per group). The average collagen content for each *Ednrb*$^{-/-}$ mouse was normalized to its wild-type littermate control for statistical comparisons. For human subjects, the average collagen content per patient sample was calculated separately from representative images of the muscularis propria and the submucosa for human subjects. For HSCR patients, each sample was normalized to the closest age- and site-matched control and ARM patient. For jejunal-ileal atresia patients, the proximal intestinal collagen content was normalized to the distal intestinal collagen content for the same patient.

Quantification of Tissue Stiffness

The BioScope II atomic force microscope (Bruker Corporation, Santa Barbara, CA) was used to quantify the mechanical stiffness of the proximal colon tissues using a colloidal probe technique. Tissues were embedded in OCT media, flash frozen at -80 °C, cryosectioned at a thickness of 10 µm, and mounted onto a poly-L-lysine-coated glass slide. A Nikon TE2000 microscope confirmed the probe's location within the muscularis propria layer. A 2.5 µm spherical colloidal probe on a soft cantilever (k = 0.24 N/m) was used to indent tissue samples by 4 µm at 0.5 Hz. The elastic modulus of each tissue specimen was obtained by fitting the force-indentation curve using a Hertz model. The elastic modulus for each *Ednrb*$^{-/-}$ mouse was normalized to its wild-type littermate control for statistical comparisons.

RNA Extraction and Bulk RNA Sequencing

The longitudinal muscle and myenteric plexus (LMMP) were isolated from proximal and distal colonic segments by microdissection of *Ednrb*$^{-/-}$ mice and their wild-type littermates (n = 4 each group). Tissues were homogenized, and RNA was isolated using the RNeasy Kit (Qiagen, Germantown, MD, USA), and bulk RNA sequencing was performed. The resultant RNA-Seq data were mapped using HISAT2 to the mouse genome build UCSC mm39. Gene expression quantification was achieved using FEATURECOUNTS (50) against the GENCODE gene model. Differential gene expression was evaluated using the R package EdgeR (51) and was further normalized using the R package RUVr4 (LRT RUVr). Significance was defined as a fold change exceeding 1.5x and FDR <0.05. Volcano plots were generated using the Enhanced Volcano package in the R statistical system. Enriched pathways were assessed via the over-representation (ORA) (52) method using the hypergeometric distribution and the MSigDB (16) v7.5.1 genesets. Additional gene ontology (GO) term analyses were performed using ShinyGO (53)

Statistical Analysis

Values are represented as mean ± standard deviation. Statistical analysis was performed using GraphPad Prism version 9.0 for Windows (GraphPad Software, La Jolla, CA) and R (version 4.4.1). Statistical significance of collagen content and tissue stiffness was compared using a two-tailed unpaired Student's *t*-test. We considered a p-value < 0.05 to be statistically significant.

Study Approval

All mice were housed in a controlled environment with a 12-hour light/dark cycle and provided access to food and water *ad libitum*. All animal-based experiments were approved by the Institutional Animal Care and Use Committees of Baylor College of Medicine and the University of Virginia.

Data Availability

Data generated or analyzed are included in the Supporting Data Values file. Sequencing data can be accessed using accession number: GSE305622

AUTHOR CONTRIBUTIONS

PCO, BAH, CM, OOO, WDS, HL, YZ, and LSC performed experiments, analyzed data, and interpreted results of experiments. SB, SGK, and LSC conceived and designed research. PCO, BAH, CM, and LSC prepared figures, drafted the manuscript. All authors edited, revised, and approved the final version of the manuscript.

BAH and PCO share first authorship based on their equal contribution to this project. First authorship was based on the amount of work contributed to the experiments, data collection, analysis, and manuscript preparation.

ACKNOWLEDGMENTS

The authors would like to thank Ana-Maria Zaske, PhD and the University of Texas Houston Atomic Force Microscopy Core for assistance with atomic force microscopy and Saad Malik for technical assistance.

GRANTS

This work is the result of NIH funding, in whole or in part, and is subject to the NIH Public Access Policy. Through acceptance of this federal funding, the NIH has been given a right to make the work publicly available in PubMed Central.

This work was funded by NIH/NIDDK K08DK133673 (to LSC), Texas Medical Center Digestive Diseases Center P30DK056338 (to LSC), the American College of Surgeons Franklin H. Martin Faculty Research Award (to LSC), the American Pediatric Surgical Association Jay Grosfeld Scholar Award (to LSC), NIH/NIGMS R01GM111808 (to SGK), and NIH/NHLBI T32HL007849 (to PCO and CM).

DISCLOSURES

None.

DISCLAIMERS

None.

REFERENCES

1. Bhave S, Arciero E, Baker C, et al. Pan-enteric neuropathy and dysmotility are present in a mouse model of short-segment Hirschsprung disease and may contribute to post-pullthrough morbidity. *J Pediatr Surg*. 2021;56(2):250-256. doi:10.1016/j.jpedsurg.2020.04.002

2. Mueller JL, Goldstein AM. The science of Hirschsprung disease: What we know and where we are headed. *Semin Pediatr Surg*. 2022;31(2):151157. doi:10.1016/j.sempedsurg.2022.151157

3. Furness JB. The enteric nervous system and neurogastroenterology. *Nat Rev Gastroenterol Hepatol*. 2012;9(5):286-294. doi:10.1038/nrgastro.2012.32

4. Nagy N, Goldstein AM. Enteric nervous system development: A crest cell's journey from neural tube to colon. *Semin Cell Dev Biol*. 2017;66:94-106. doi:10.1016/j.semcdb.2017.01.006

5. Montalva L, Cheng LS, Kapur R, et al. Hirschsprung disease. *Nat Rev Dis Primer*. 2023;9(1):54. doi:10.1038/s41572-023-00465-y

6. Anderson RB, Newgreen DF, Young HM. Neural Crest and the Development of the Enteric Nervous System. In: Saint-Jeannet JP, ed. *Neural Crest Induction and Differentiation*. Vol 589. Advances in Experimental Medicine and Biology. Springer US; 2006:181-196. doi:10.1007/978-0-387-46954-6_11

7. Goldstein AM, Hofstra RMW, Burns AJ. Building a brain in the gut: development of the enteric nervous system. *Clin Genet*. 2013;83(4):307-316. doi:10.1111/cge.12054

8. Soret R, Mennetrey M, Bergeron KF, et al. A collagen VI–dependent pathogenic mechanism for Hirschsprung's disease. *J Clin Invest*. 2015;125(12):4483-4496. doi:10.1172/JCI83178

9. Amiel J. Hirschsprung disease, associated syndromes, and genetics: a review. *J Med Genet*. 2001;38(11):729-739. doi:10.1136/jmg.38.11.729

10. Klein M, Varga I. Hirschsprung's Disease—Recent Understanding of Embryonic Aspects, Etiopathogenesis and Future Treatment Avenues. *Medicina (Mex)*. 2020;56(11):611. doi:10.3390/medicina56110611

11. Heuckeroth RO. Hirschsprung disease — integrating basic science and clinical medicine to improve outcomes. *Nat Rev Gastroenterol Hepatol*. 2018;15(3):152-167. doi:10.1038/nrgastro.2017.149

12. Rintala RJ, Pakarinen MP. Long-term outcomes of Hirschsprung's disease. *Semin Pediatr Surg*. 2012;21(4):336-343. doi:10.1053/j.sempedsurg.2012.07.008

13. Bonnans C, Chou J, Werb Z. Remodelling the extracellular matrix in development and disease. *Nat Rev Mol Cell Biol*. 2014;15(12):786-801. doi:10.1038/nrm3904

14. Gao N, Wang J, Zhang Q, et al. Aberrant Distributions of Collagen I, III, and IV in Hirschsprung Disease. *J Pediatr Gastroenterol Nutr*. 2020;70(4):450-456. doi:10.1097/MPG.0000000000002627

15. Nishida S, Yoshizaki H, Yasui Y, Kuwahara T, Kiyokawa E, Kohno M. Collagen VI suppresses fibronectin-induced enteric neural crest cell migration by downregulation of focal adhesion proteins. *Biochem Biophys Res Commun*. 2018;495(1):1461-1467. doi:10.1016/j.bbrc.2017.11.184

16. Parikh DH, Tam PK, Van Velzen D, Edgar D. Abnormalities in the distribution of laminin and collagen type IV in Hirschsprung's disease. *Gastroenterology*. 1992;102(4 Pt 1):1236-1241.

17. Lotakis DM, Dheer R, Dame MK, et al. A Pilot Study: Transcriptional Profiling, Functional Analysis, and Organoid Modeling of Intestinal Mucosa in Hirschsprung Disease. *J Pediatr Surg*. 2023;58(6):1164-1169. doi:10.1016/j.jpedsurg.2023.02.020

18. Chevalier NR, Gazquez E, Bidault L, et al. How Tissue Mechanical Properties Affect Enteric Neural Crest Cell Migration. *Sci Rep*. 2016;6(1):20927. doi:10.1038/srep20927

19. Coyle D, O'Donnell AM, Gillick J, Puri P. Altered neurotransmitter expression profile in the ganglionic bowel in Hirschsprung's disease. *J Pediatr Surg*. 2016;51(5):762-769. doi:10.1016/j.jpedsurg.2016.02.018

20. Zaitoun I, Erickson CS, Barlow AJ, et al. Altered neuronal density and neurotransmitter expression in the ganglionated region of *Ednrb* null mice: implications for Hirschsprung's disease. *Neurogastroenterol Motil*. 2013;25(3). doi:10.1111/nmo.12083

21. The Jackson Lab. B6;129-Ednrbtm1Ywa/J. B6;129-Ednrbtm1Ywa/J

22. Kanehisa Laboratories. Focal adhesion - Mus musculus (house mouse). Kyoto Encyclopedia of Genes and Genomes (KEGG) database. https://www.kegg.jp/entry/mmu04510

23. Kanehisa Laboratories. ECM-receptor interaction - Mus musculus (house mouse). Kyoto Encyclopedia of Genes and Genomes (KEGG) database. https://www.kegg.jp/pathway/mmu04512

24. Kanehisa Laboratories. Neuroactive ligand-receptor interaction - Mus musculus (house mouse). Kyoto Encyclopedia of Genes and Genomes (KEGG) database. https://www.kegg.jp/pathway/mmu04080

25. RT^2 Profiler™ PCR Array Mouse Extracellular Matrix & Adhesion Molecules. GeneGlobe. QIAGEN. https://geneglobe.qiagen.com/us/product-groups/rt2-profiler-pcr-arrays/PAMM-013Z

26. RT^2 Profiler™ PCR Array Mouse Fibrosis. GeneGlobe. QIAGEN. https://geneglobe.qiagen.com/us/product-groups/rt2-profiler-pcr-arrays/PAMM-120Z

27. Sergi C. Hirschsprung's disease: Historical notes and pathological diagnosis on the occasion of the 100(th) anniversary of Dr. Harald Hirschsprung's death. *World J Clin Pediatr*. 2015;4(4):120-125. doi:10.5409/wjcp.v4.i4.120

28. Celayir A, Çetiner H, Ağartan CA, Günaydın R, Celayir A. A note on the history of Hirschsprung's disease, and an over 120 years apology. *Pediatr Surg Int*. 2025;41(1):153. doi:10.1007/s00383-025-06003-z

29. Cheng LS, Schwartz DM, Hotta R, Graham HK, Goldstein AM. Bowel dysfunction following pullthrough surgery is associated with an overabundance of nitrergic neurons in Hirschsprung disease. *J Pediatr Surg*. 2016;51(11):1834-1838. doi:10.1016/j.jpedsurg.2016.08.001

30. Brooks LA, Fowler KL, Veras LV, Fu M, Gosain A. Resection margin histology may predict intermediate-term outcomes in children with rectosigmoid Hirschsprung disease. *Pediatr Surg Int*. 2020;36(8):875-882. doi:10.1007/s00383-020-04689-x

31. Parikh DH, Tam PK, Van Velzen D, Edgar D. Abnormalities in the distribution of laminin and collagen type IV in Hirschsprung's disease. *Gastroenterology*. 1992;102(4 Pt 1):1236-1241.

32. Fujiwara N, Nakazawa-Tanaka N, Miyahara K, Arikawa-Hirasawa E, Akazawa C, Yamataka A. Altered expression of laminin alpha1 in aganglionic colon of endothelin receptor-B null mouse model of Hirschsprung's disease. *Pediatr Surg Int*. 2018;34(2):137-141. doi:10.1007/s00383-017-4180-6

33. Nagy N, Barad C, Graham H, et al. Sonic hedgehog controls enteric nervous system development by patterning the extracellular matrix. *Development*. Published online January 1, 2015:dev.128132. doi:10.1242/dev.128132

34. Wu H, Yu Y, Huang H, et al. Progressive Pulmonary Fibrosis Is Caused by Elevated Mechanical Tension on Alveolar Stem Cells. *Cell*. 2020;180(1):107-121.e17. doi:10.1016/j.cell.2019.11.027

35. Henderson NC, Rieder F, Wynn TA. Fibrosis: from mechanisms to medicines. *Nature*. 2020;587(7835):555-566. doi:10.1038/s41586-020-2938-9

36. Chaudhuri O, Cooper-White J, Janmey PA, Mooney DJ, Shenoy VB. Effects of extracellular matrix viscoelasticity on cellular behaviour. *Nature*. 2020;584(7822):535-546. doi:10.1038/s41586-020-2612-2

37. Long Y, Niu Y, Liang K, Du Y. Mechanical communication in fibrosis progression. *Trends Cell Biol*. 2022;32(1):70-90. doi:10.1016/j.tcb.2021.10.002

38. Courbot O, Elosegui-Artola A. The role of extracellular matrix viscoelasticity in development and disease. *Npj Biol Phys Mech*. 2025;2(1):10. doi:10.1038/s44341-025-00014-6

39. Dzobo K, Dandara C. The Extracellular Matrix: Its Composition, Function, Remodeling, and Role in Tumorigenesis. *Biomimetics*. 2023;8(2):146. doi:10.3390/biomimetics8020146

40. Subbarayan D, Singh M, Khurana N, Sathish A. Histomorphological Features of Intestinal Atresia and its Clinical Correlation. *J Clin Diagn Res JCDR*. 2015;9(11):EC26-29. doi:10.7860/JCDR/2015/13320.6838

41. Leung A, Crombleholme TM, Keswani SG. Fetal wound healing: implications for minimal scar formation. *Curr Opin Pediatr*. 2012;24(3):371-378. doi:10.1097/MOP.0b013e3283535790

42. Balaji S, Wang X, King A, et al. Interleukin-10-mediated regenerative postnatal tissue repair is dependent on regulation of hyaluronan metabolism via fibroblast-specific STAT3 signaling. *FASEB J Off Publ Fed Am Soc Exp Biol*. 2017;31(3):868-881. doi:10.1096/fj.201600856R

43. Mack M. Inflammation and fibrosis. *Matrix Biol J Int Soc Matrix Biol*. 2018;68-69:106-121. doi:10.1016/j.matbio.2017.11.010

44. Santos A, Lagares D. Matrix Stiffness: the Conductor of Organ Fibrosis. *Curr Rheumatol Rep*. 2018;20(1):2. doi:10.1007/s11926-018-0710-z

45. Nho RS, Ballinger MN, Rojas MM, Ghadiali SN, Horowitz JC. Biomechanical Force and Cellular Stiffness in Lung Fibrosis. *Am J Pathol*. 2022;192(5):750-761. doi:10.1016/j.ajpath.2022.02.001

46. Viji Babu PK, Radmacher M. Mechanics of Brain Tissues Studied by Atomic Force Microscopy: A Perspective. *Front Neurosci*. 2019;13:600. doi:10.3389/fnins.2019.00600

47. Chevalier NR, Peaucelle A, Guilbert T, Bourdoncle P, Xi W. The enteric nervous system is 10 times stiffer than the brain. *Biophys J*. Published online May 2025:S0006349525002899. doi:10.1016/j.bpj.2025.05.010

48. Swift J, Ivanovska IL, Buxboim A, et al. Nuclear lamin-A scales with tissue stiffness and enhances matrix-directed differentiation. *Science*. 2013;341(6149):1240104. doi:10.1126/science.1240104

49. Stewart DC, Berrie D, Li J, et al. Quantitative assessment of intestinal stiffness and associations with fibrosis in human inflammatory bowel disease. Singh SR, ed. *PLOS ONE*. 2018;13(7):e0200377. doi:10.1371/journal.pone.0200377

50. Liao Y, Smyth GK, Shi W. featureCounts: an efficient general purpose program for assigning sequence reads to genomic features. *Bioinformatics*. 2014;30(7):923-930. doi:10.1093/bioinformatics/btt656

51. Robinson MD, McCarthy DJ, Smyth GK. edgeR : a Bioconductor package for differential expression analysis of digital gene expression data. *Bioinformatics*. 2010;26(1):139-140. doi:10.1093/bioinformatics/btp616

52. Subramanian A, Tamayo P, Mootha VK, et al. Gene set enrichment analysis: A knowledge-based approach for interpreting genome-wide expression profiles. *Proc Natl Acad Sci*. 2005;102(43):15545-15550. doi:10.1073/pnas.0506580102

53. Ge SX, Jung D, Yao R. ShinyGO: a graphical gene-set enrichment tool for animals and plants. Valencia A, ed. *Bioinformatics*. 2020;36(8):2628-2629. doi:10.1093/bioinformatics/btz931

FIGURE LEGENDS

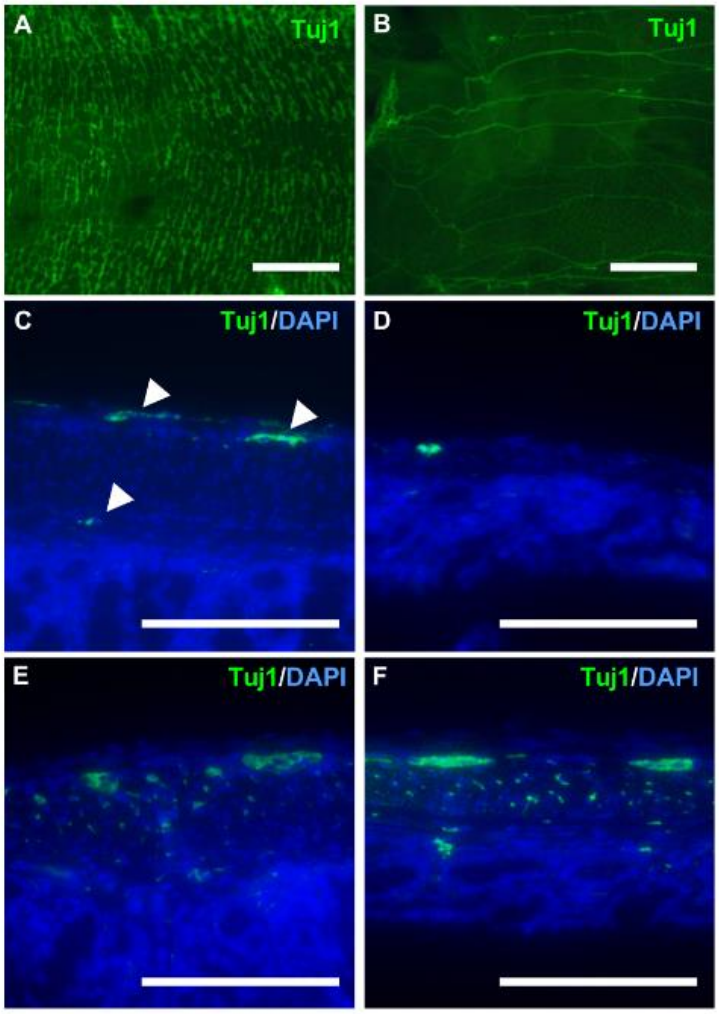

Figure 1: Reduced ganglion and neuronal density in the distal colon of HSCR mice

Aganglionosis of in the distal *Ednrb*$^{-/-}$ colon was confirmed by immunohistochemistry for the pan-neuronal marker, Tuj1. Whole mount immunohistochemistry of the muscularis propria demonstrated abundant innervation of the ganglionic segment (A) and sparse innervation of the aganglionic segment (B) in the *Ednrb*$^{-/-}$ mouse. Similarly, tissue sections of the proximal colon in the *Ednrb*$^{-/-}$ mouse confirmed the presents of myenteric and submucosal ganglia (C; white arrowheads) whereas sparse and small ganglia are seen in the distal colon (D). In contrast, equivalent segments of the proximal and distal colon in the WT (*Ednrb*$^{+/+}$) littermate demonstrate abundant ganglia in both proximal and distal segments (E, F). Scale bar is 500 µm for A-B and is 100 µm for C-F.

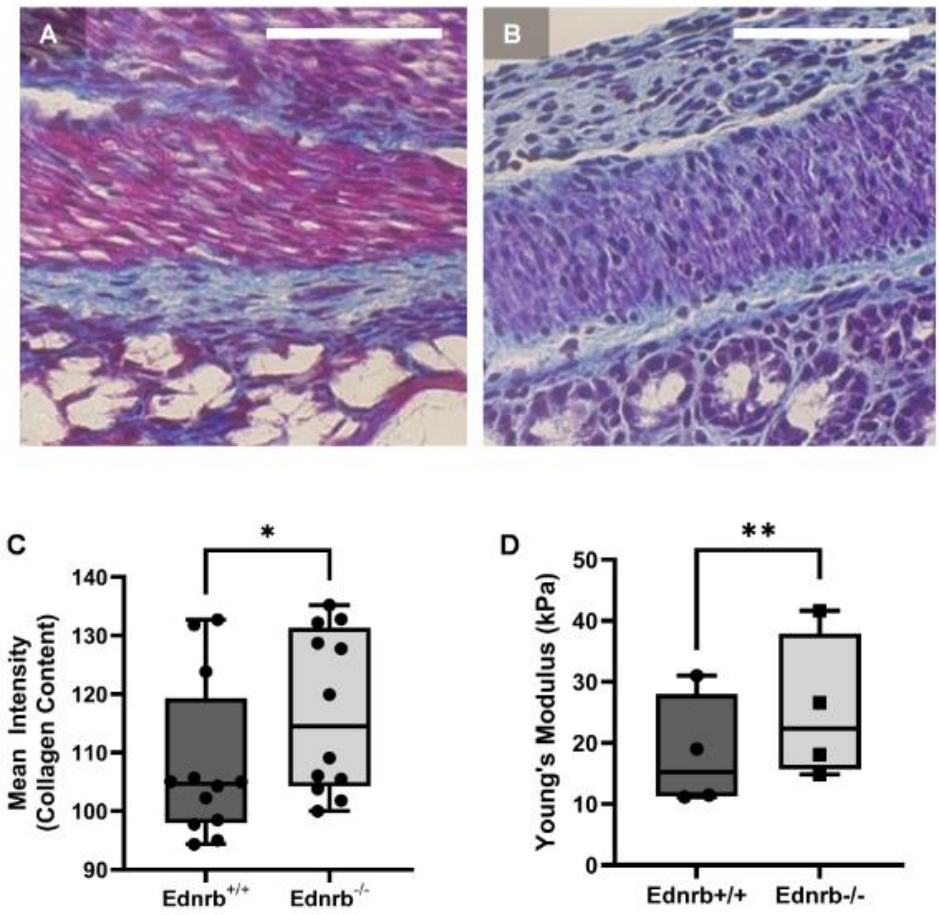

Figure 2: HSCR mice have stiff and fibrotic proximal ganglionic colon

Representative images of the proximal ganglionic colon in wild-type (*Ednrb*$^{+/+}$, A) and HSCR (*Ednrb*$^{-/-}$,B) mice are shown with Masson's trichrome staining to quantify fibrosis. Atomic force microscopy was used to quantify stiffness. When normalized to age-matched wild-type littermates (n=12), HSCR (n=12) mice had significantly greater collagen content in the muscularis propria (C; * is p = 0.006). HSCR (n=4) mice also had significantly greater stiffness (D; ** is p = 0.0003) when compared to wild-type littermates (n=4). Each data point represents the average of at least 5 fields of view of 1 biological replicate. Student's 2-tailed *t* test used for statistical analysis. Scale bar is 100 μm for A-B.

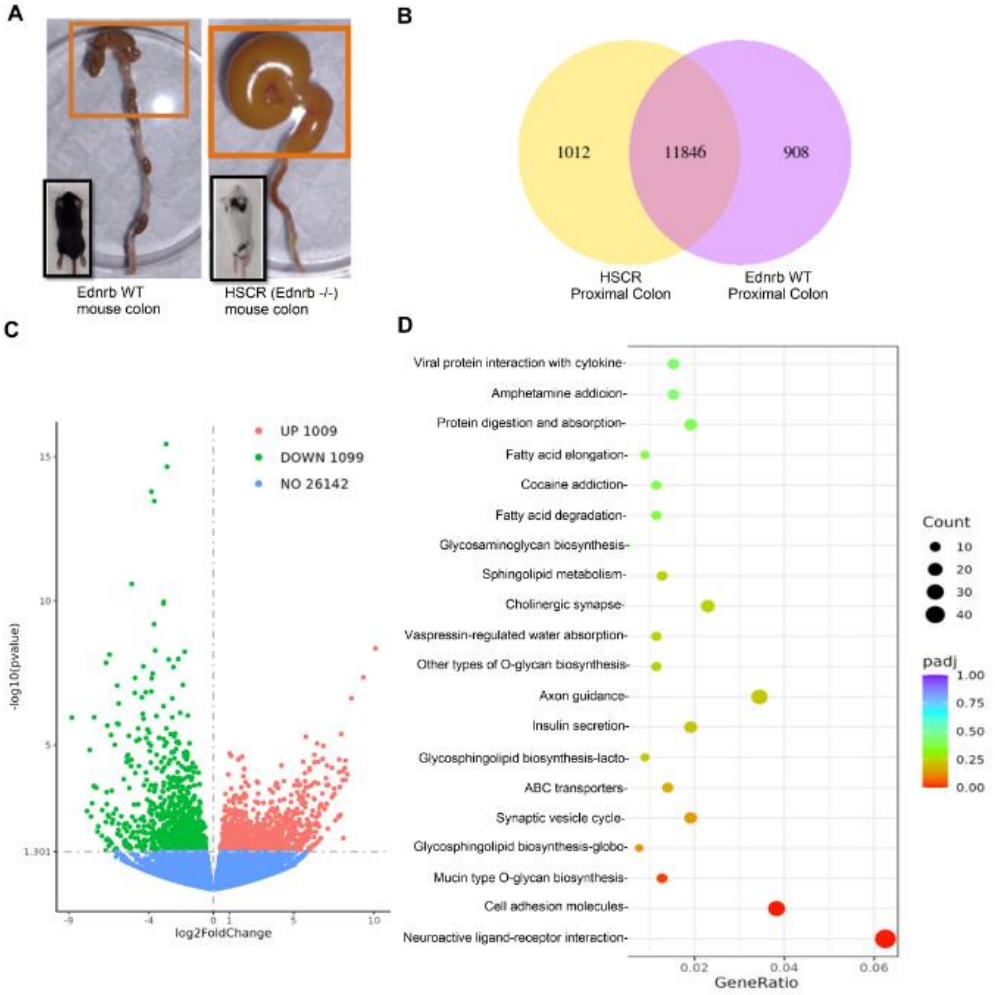

Figure 3: Differential gene expression in proximal ganglionic colon.

The longitudinal muscle and myenteric plexus from the proximal colons of HSCR (*Ednrb*$^{-/-}$) and wild-type (*Ednrb*$^{+/+}$) littermates were analyzed for differences in RNA expression (A). Venn diagram comparing differentially expressed genes (DEGs) in the proximal colon of HSCR and WT mice identified 1,012 uniquely dysregulated genes in HSCR and 908 in WT with 11,846 genes in common between both groups (B). Volcano plot of RNA sequencing shows that 2,108 genes were differentially expressed with 1,009 upregulated genes and 1,099 downregulated genes (C). Lollipop plot of top enriched KEGG pathways among DEGs (D).

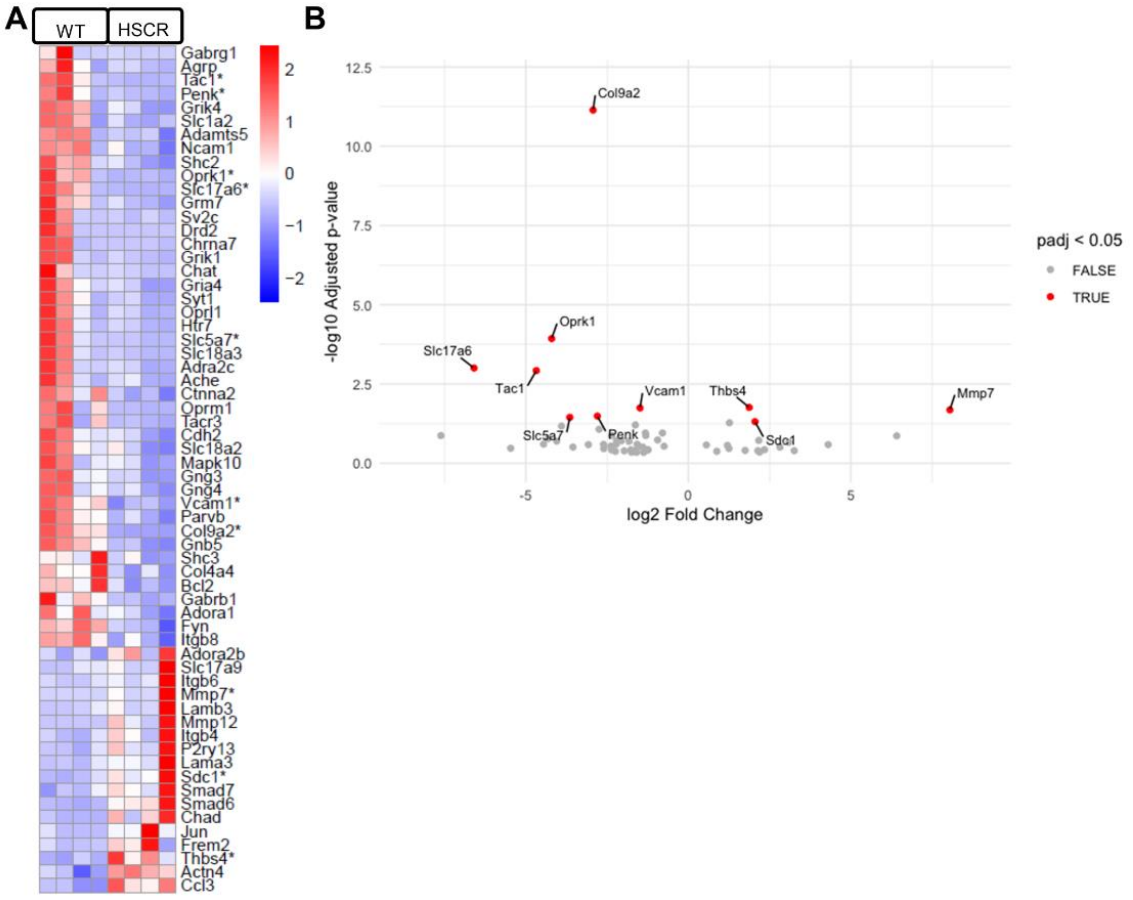

Figure 4: Extracellular matrix-related differential gene expression in proximal ganglionic colon

Heatmap comparison of differentially expressed genes involved in focal adhesion, fibrosis, ECM–receptor interaction, and neuroactive ligand–receptor pathways in the proximal colon of HSCR and wild-type mice (D; * signifies padj <0.05) (A). Volcano plot showing Log2FC of 10 statistically significant genes (padj < 0.05) involved in fibrosis and extracellular matrix (C).

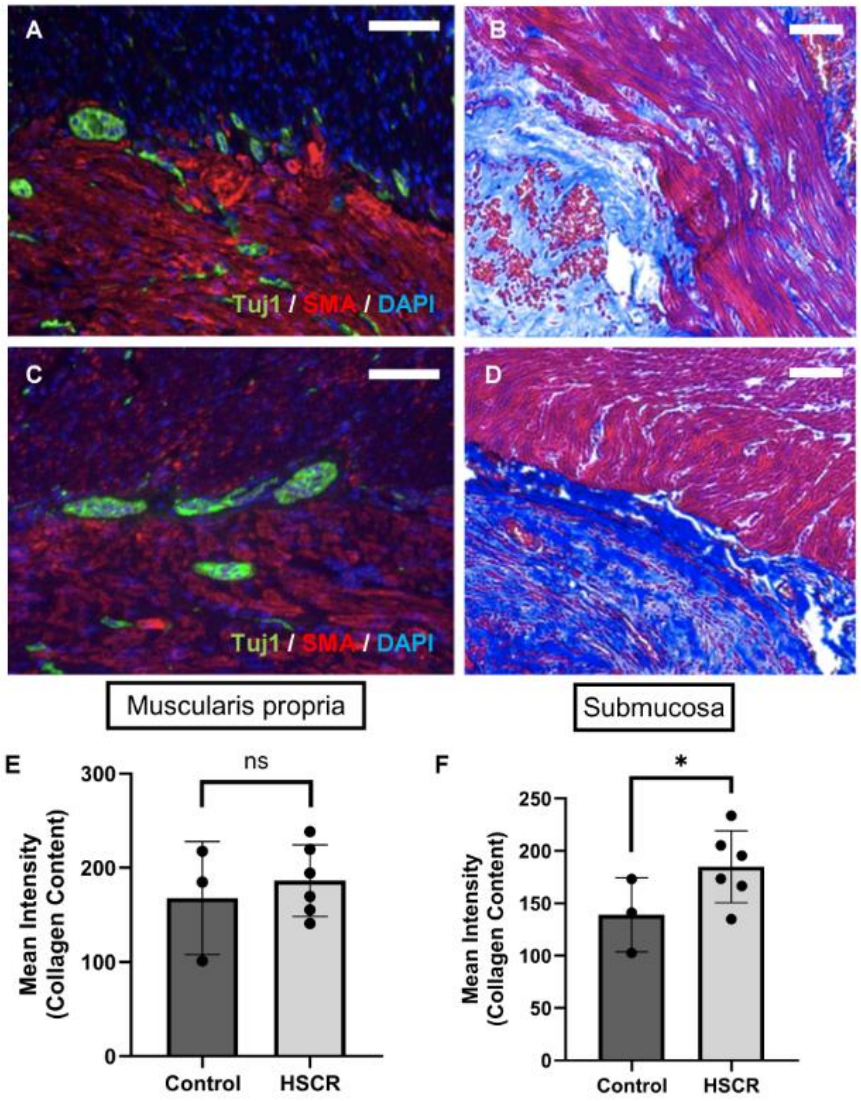

Figure 5: Human patients with HSCR have increased fibrosis in ganglionic intestine

Representative immunofluorescent images of the proximal ganglionic intestine in healthy control patients (A) and in patients with Hirschsprung disease (HSCR; C) confirms the presence of normal ganglion cells within the muscularis propria (Tuj1 is a pan-neuronal marker, SMA is smooth muscle actin, DAPI denotes cell nuclei). Masson's trichrome staining was used to compare collagen content between control patients (B) and HSCR patients (D). Patients with HSCR (n=6) had increased fibrosis in the muscularis propria (E; $p = 0.08$) and significantly increased fibrosis in the submucosa (F; * is $p = 0.0002$) when normalized to age- and site-matched controls (n=3). Each data point represents the average of at least 5 fields of view of 1 biological replicate. Student's 2-tailed *t* test used for statistical analysis. Scale bar is 100 μm for A-D

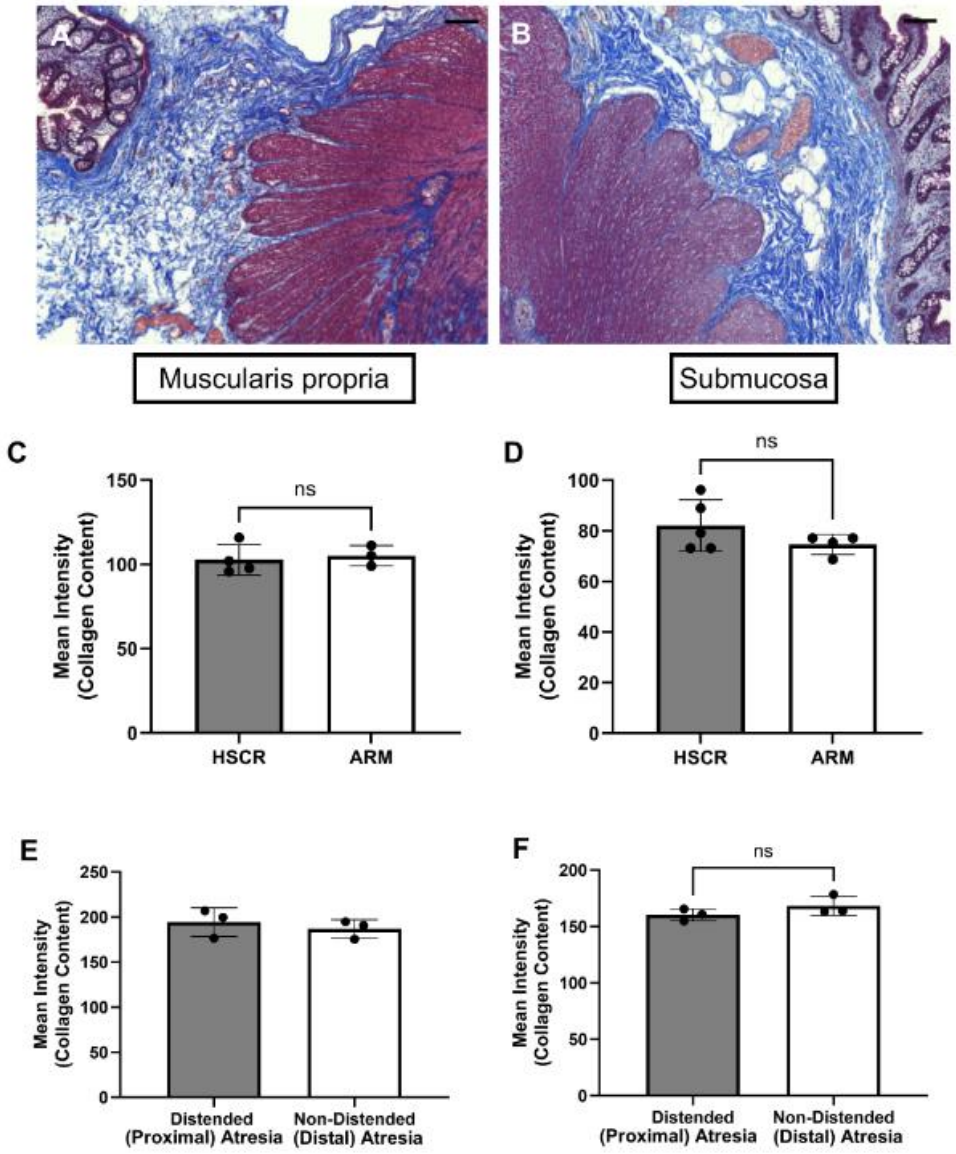

Figure 6: No difference in fibrosis in age-matched HSCR, ARM, and intestinal atresia patients

Representative Masson's trichrome staining of proximal ganglionated intestinal tissues from age-matched HSCR (A) and ARM (B) patients. No notable difference in fibrosis was observed between HSCR (n=4) and ARM (n=3) patients in either the muscular propria or the submucosa (C-D). Patients with jejunoileal atresia had no notable difference in fibrosis between distended proximal and non-distended distal intestinal segments (E-F; n=3 each). Each data point represents the average of at least 5 fields of view of 1 biological replicate. Student's 2-tailed *t* test used for statistical analysis. Scale bar is 100 μm for A-B.

TABLES

Table 1. Human patient specimens

Age	Sex	Diagnosis	Tissue Site	Pair ID (letter)
2-year-old	Male	Control (trauma)	Ileum	a
13-year-old	Male	Control (trauma)	Ileum	b
13-year-old	Female	Control (trauma)	Sigmoid colon	c
1-year-old	Female	Hirschsprung disease	Ileum	a
3-year-old	Male	Hirschsprung disease	Ileum	a
5-year-old	Male	Hirschsprung disease	Ileum	a
13-year-old	Male	Hirschsprung disease	Sigmoid colon	c
13-year-old	Male	Hirschsprung disease	Ileum	b
14-year-old	Male	Hirschsprung disease	Ileum	b
3-day-old	Male	Jejunal-ileal atresia	Jejunum	-
4-day-old	Male	Jejunal-ileal atresia	Ileum	-
2-month-old	Female	Jejunal-ileal atresia	Jejunum	-
9-day-old	Male	Hirschsprung disease	Rectum	f
14-day-old	Female	Hirschsprung disease	Colon	f
2-month-old	Male	Hirschsprung disease	Rectum + Colon	e
17-month-old	Male	Hirschsprung disease	Rectum + Colon	d
2-year-old	Male	Hirschsprung disease	Rectum + Colon	d
3-week-old	Female	Anorectal Malformation	Rectum	f
3-month-old	Male	Anorectal Malformation	Rectum	e
9-month-old	Male	Anorectal Malformation	Colon	d
10-month-old	Male	Anorectal Malformation	Rectum	d

SUPPLEMENTAL MATERIAL

Supplemental Table 1:

List of all differentially expressed genes in the proximal colon of wildtype and HSCR littermates. DOI: 10.25833/bdr0-kf36

Supplemental Table 2:

Genes involved in fibrosis, ECM-receptor interaction, focal adhesion, and neuroactive-receptor ligand pathways in Mus musculus (house mouse) (22–24) that were queried for heat map shown in Figure 4. DOI: 10.25833/bdr0-kf36